

Response to the Referees

Response to Anonymous Referee #1

(1) Comments from Referee #1

Interactive comment on “Prediction of gas/particle partitioning of polybrominated diphenyl ethers (PBDEs) in global air: a theoretical study” by Y.-F. Li et al.

Anonymous Referee #1

Received and published: 2 December 2014

Review of Li et al. on PBDEs in air

This paper builds on a recent publication by the authors cited on line 717. That publication provides a comprehensive set of data (700 pairs) on partitioning of PBDEs between gas (G) and particle (P) (aerosol) phases, mainly in China and over a wide range in temperature (-22 to 38 deg C). They test the dependence of the P/G partition coefficient K_p on the octanol-air partition coefficient K_{oa} . The important conclusion is that equilibrium appears to apply at $\log K_{oa}$ up to about 10 then K_p tends to level off and becomes constant at $\log K_{oa}$ above about 12. This is novel and important information. They develop several empirical regression equations. They claim that the constant K_p regime is due to “saturation”. I have a problem with their use of that word. To me, saturation implies an equilibrium state between two phases or, if one of the phases is a pure substance, a solubility limit. Clearly conditions are far from equilibrium or saturation. They recognize that in the intermediate regime conditions are “non equilibrium” but steady state. In my opinion there is an equilibrium region, a steady state region and between them lies a transition region.

The introduction is essentially a restatement of the work in the first paper. I find their derivation and discussion very long and convoluted and difficult to understand. This is not helped by reference to extensive Supplementary information with 18 figures.

They cite a paper by Rissler et al. On the kinetics of G - P transfer. I would have expected other citations especially to the texts by Seinfeld & Pandis and Finlayson Pitts and Pitts.

I believe that a much shorter, higher impact and more understandable paper could be written that would do better justice to their excellent empirical studies. My suggestion is major revision.

(2) Author's response and (3) author's changes in manuscript

This Review is the same as the one made by Anonymous Referee #1 under the initial manuscript evaluation before the paper was accepted for publication on the Atmospheric Chemistry and Physics Discussions (ACPD) website. We have responded these comments and some of their suggestions have been taken to revise our manuscript published on the ACPD website already, as shown below.

This paper builds on a recent publication by the authors cited on line 717. That publication provides a comprehensive set of data (700 pairs) on partitioning of PBDEs between gas (G) and particle (P) (aerosol) phases, mainly in China and over a wide range in temperature (-22 to 38 deg C). They test the dependence of the P/G partition coefficient K_p on the octanol-air partition coefficient K_{oa} . The important conclusion is that equilibrium appears to apply at $\log K_{oa}$ up to about 10 then K_p tends to level off and becomes constant at $\log K_{oa}$ above about 12. This is novel and important information. They develop several empirical regression equations. They claim that the constant K_p regime is due to “saturation”. I have a problem with their use of that word. To me, saturation implies an equilibrium state between two phases or, if one of the phases is a pure substance, a solubility limit. Clearly conditions are far from equilibrium or saturation.

RE: Agree! The term “saturation (SA)” was changed to “maximum partition (MP)” in the revised manuscript.

They recognize that in the intermediate regime conditions are “non equilibrium” but steady state. In my opinion there is an equilibrium region, a steady state region and between them lies a transition region.

RE: We do not agree. “Transition region” means the region is neither equilibrium nor steady state. Actually all the three regions (equilibrium, non-equilibrium, and the maximum partition region) are *steady state*, since all of them are solutions of the steady equation (9) ($N_{G-P} = N_{P-G} + N_{P-S}$).

The introduction is essentially a restatement of the work in the first paper. I find their derivation and discussion very long and convoluted and difficult to understand. This is not helped by reference to extensive Supplementary information with 18 figures.

RE: The introduction presents the development of the study on gas-particle partitioning behavior for SVOC. Each equation (from (1) to (8)) represents a step forward in the development, which is important to lead the objectives of our present study.

They cite a paper by Rissler et al. On the kinetics of G - P transfer. I would have expected other citations especially to the texts by Seinfeld & Pandis and Finlayson Pitts and Pitts.

RE: We cite the paper by Rissler et al. only for the mean diameter of 0.1 m for aerosols.

I believe that a much shorter, higher impact and more understandable paper could be written that would do better justice to their excellent empirical studies. My suggestion is major revision.

RE: Both the paper and the Supplementary were shortened.

Response to Anonymous Referee #2

(1) Comments from Referees #2

Interactive comment on “Prediction of gas/particle partitioning of polybrominated diphenyl ethers (PBDEs) in global air: a theoretical study” by Y.-F. Li et al.

Anonymous Referee #2

Received and published: 15 October 2014

A steady-state model is developed in this study to model gas/particle participation of PBDEs in air. In addition to the chemical transfer from gas to particles, the competing dry and wet depositions of particles are taken into account in quantifying gas/particle participation. The study concludes that the equilibrium state is a special case of the steady state when particle depositions are negligible relative to gaseous transfer. The steady-state model shows better performance in fitting field measurements than the equilibrium model published previously. The authors present a list of equations to substantiate the development of the steady-state model. The findings are novel and could be applied to model environmental behaviour and fate of PBDEs. The manuscript is recommended for publication in ACP.

1. Line 5 on page 23418, defining K_{pm} is not really necessary since this parameter is not used in any equations. The readers can be easily confused by so many newly defined parameters such as K_{pr} , K_{pe} or K_{pp} .
2. Line 25-28 on page 23418, f_{OM} is not a constant and it varies significantly from one site to another, similar to TSP. As such, f_{OM} needs to be monitored as well in real environment.
3. Line 12 on page 23420, the parameters A and B in Eq. (8) vary among different PBDE congeners. Consider deriving another equation of $\log K_{pp}(t)$, similar to Eq. (8), since ambient temperature is more readily available than $\log K_{oa}$, and can thus be readily used by modellers.
4. Line 16-18 on page 23441, consider re-wording this sentence.
5. Line 25 on page 23424, it appears arbitrary to introduce the constant C in Eq. (21). What is the physical meaning of C? How could this parameter be subjectively changed from 5 to 50 at Waliguan site? A bit more explanation and justification is needed here for the constant C.
6. Typos: (1). Line 4 on page 23416, replace ‘routs’ with ‘routes’. (2). Line 2 and 4 on page 23419, consider replacing ‘Eq. (3)’ with ‘Eq. (2)’. (3). Line 21 on page

23419, replace ‘are’ with ‘is’. (4). Line 4-7 on page 23440, consider replacing ‘steady’ with ‘steady state’. (5). Line 12 on page 23441, replace ‘planed’ with ‘planned’.

(2) Author's response and (3) author's changes in manuscript

General

We thank the Referee #2 for his remark on the novelty of our paper, the support to publish this paper in ACP, and also the comments on the weak points and errors made in the paper. We response these comments in the following.

1. In this paper, many new parameters of K_P , including K_{PM} , K_{PR} , K_{PE} , and K_{PS} , have been defined for establishing the steady-state model for G/P partitioning study. K_{PM} is directly calculated using the monitoring data. Although K_{PM} has not been used in any equation in the paper, but it is used to derive Eq. (2) and also in Figures 5, S11, S13, and S15.
2. In our study, the value of f_{OM} was assumed as 0.1 as suggested by Mackay 2001. Although the real values of f_{OM} at sampling sites were most likely different from 0.1, but this did not affect the application of the steady-state equations, as discussed in Section “4.5 The limitation of application”. Actually we did the sensitivity analysis for parameter f_{OM} , and it was found that the final results are not sensitive to the variation of the parameter f_{OM} . In the future, however, we will try to monitor the values of f_{OM} .
3. We derived the equation to calculate $\log K_{PP}(t)$ in our previous paper (Li and Jia, 2014), which has the form $\log K_{PP}(t) = (0.011A - 0.135)t - 2.74B/(t+273) + 0.263A + 0.011B - 5.006$

Reference: Li Y. F. and Jia, H. L.: Prediction of Gas/Particle Partition Quotients of Polybrominated Diphenyl Ethers (PBDEs) in north temperate zone air: An empirical approach, Ecotoxic. Environ. Safety, 108, 65-71, 2014.

4. “As equilibrium is an idealized scenario not presenting in real environment, the steady state discussed here is also an ideal one, since only dry and wet depositions were discussed.” has been changed to “It should be borne in mind that the steady state discussed here is an idealized scenario since only dry and wet depositions were discussed in the study, other factors, such as humidity and artifacts, will also play roles to a certain extent to affect the G/P partitioning.”
5. “The value of C will be determined later” has been changed to “Thus the term CB_a is the chemical's molecular diffusivity for the particle film in air, and the value of C will be determined later”. More discussions on C can be found in the section

“4.5 The limitation of applications”.

6. All typos except Typo (2) have been corrected. For Typo (2), we didn't make the replacement, because Eq. (3) is right.

1 **Prediction of gas/particle partitioning of polybrominated
2 diphenyl ethers (PBDEs) in global air: A theoretical study**

3 Yi-Fan Li^{1,2,3}, Wan-Li Ma¹, Meng Yang²

4

5 ¹ International Joint Research Center for Persistent Toxic Substances (IJRC-PTS), State Key
6 Laboratory of Urban Water Resource and Environment/School of Municipal and
7 Environmental Engineering, Harbin Institute of Technology, Harbin 150090, P. R. China

8 ² IJRC-PTS, Dalian Maritime University, Dalian, 116026, P. R. China

9 ³ IJRC-PTS-NA, Toronto, Ontario, M2N 6X9, Canada

10

11 Correspondence and requests for materials should be addressed to YFL (email:
12 ijrc_pts_paper@yahoo.com)

13

14 **Abstract**

15 Gas/particle (G/P) partitioning for ~~most~~-semivolatile organic compounds (SVOCs)
16 is an important process that primarily governs their atmospheric fate, long-range atmospheric
17 transport ~~potential~~, and their routes to enter human body. All previous studies on this issue
18 have ~~been~~-hypothetically ~~derived from~~based on equilibrium conditions, the results of which
19 do not predict results from monitoring studies well in most cases. In this study, a *steady-state*
20 model instead of an equilibrium-state model for the investigation of the G/P partitioning
21 behavior for polybrominated diphenyl ethers (PBDEs) was established, and an equation for
22 calculating the partition coefficients under *steady state* (K_{PS}) for PBDE congeners ($\log K_{PS} =$
23 $\log K_{PE} + \log \alpha$) was developed, in which an equilibrium term ($\log K_{PE} = \log K_{OA} + \log f_{OM} - 11.91$,
24 where f_{OM} is organic matter content of the particles) and a nonequilibrium term ($\log \alpha$, ~~mainly~~
25 caused by dry and wet depositions of particles), both being functions of $\log K_{OA}$ (octanol-air
26 partition coefficient), are included. It was found that ~~and~~ the equilibrium is a special case of
27 *steady state* when the nonequilibrium term equals to zero. A criterion to classify the
28 equilibrium and nonequilibrium status for PBDEs was also established using two threshold
29 values of $\log K_{OA}$, $\log K_{OA1}$ and $\log K_{OA2}$, which divide the range of $\log K_{OA}$ into 3 domains:
30 equilibrium, nonequilibrium, and maximum partition domains; and accordingly, two
31 threshold values of temperature t , t_{TH1} when $\log K_{OA} = \log K_{OA1}$ and t_{TH2} when $\log K_{OA} =$
32 $\log K_{OA2}$, were identified, which divide the range of temperature also into the same 3 domains
33 for each PBDE congener. We predicted the existence of the maximum partition domain (the
34 values of $\log K_{PS}$ reach a maximum constant of -1.53) that every PBDE congener can reach
35 when $\log K_{OA} \geq \log K_{OA2}$, or $t \leq t_{TH2}$. The novel equation developed in this study was applied
36 to predict the G/P partition coefficients of PBDEs for the published monitoring data
37 worldwide, including Asia, Europe, North America, and the Arctic, and the results matched
38 well with all the monitoring data, except those obtained at e-waste sites due to the

39 unpredictable PBDE emissions at these sites. This study provided evidence that, the newly
40 developed *steady-state*-based equation is superior to the equilibrium-state-based equation that
41 has been used in describing the G/P partitioning behavior in decades. We suggest that, the
42 investigation on G/P partitioning behavior for PBDEs should be based on *steady state*, not
43 equilibrium state, and equilibrium is just a special case of *steady state* when nonequilibrium
44 factors can be ignored. We also believe that our new equation provides a useful tool for
45 environmental scientists in both monitoring and modeling research on G/P partitioning for
46 PBDEs and can be extended to predict G/P partitioning behavior for other SVOCs as well.

47

48

49 1 Introduction

50 Atmospheric transport is a major mechanism to move ~~most~~-semivolatile organic
51 compounds (SVOCs), including persistent organic pollutants (POPs), from
52 source regions to other remote places, including Arctic and Antarctic, where these
53 chemicals have never been produced and used (Barrie et al. 1992; Macdonald et al.
54 2000; Li et al. 1998; Li and Bidleman, 2003; Eckhardt and Manø 2007). The gas/particle
55 (also called aerosol) (G/P) partitioning for SVOCs is a very important process that
56 primarily governs their atmospheric fate (Lohmann et al., 2000), since wet and dry
57 depositions and other processes act differently on gaseous and particulate SVOCs, thus
58 affecting the efficiency and scope of their long-range atmospheric transport and fate
59 (Bidleman, 1988). In addition, SVOCs are an important class of indoor pollutants that are
60 of great health concern to humans (Weschler and Nazaroff, 2008). The gaseous and
61 particulate SVOCs have different routes to enter human body, and therefore the
62 ~~gas~~G/particle-P partitioning for SVOCs has a significant influence on human exposure
63 (Weschler, 2003).

64 The G/P partitioning behavior of SVOCs, K_P , is commonly defined as (Yamasaki et al.
65 1982, Pankow 1991, Pankow and Bidleman 1991)

$$66 \quad K_P = (C_P/TSP)/C_G \quad (1)$$

67 where C_G and C_P are concentrations of SVOCs in gas- and particle-phases (both in pg m^{-3} of
68 air), respectively, and TSP is the concentration of total suspended particle in air ($\mu\text{g m}^{-3}$).
69 Thus K_P has a unit of $\text{m}^3 \mu\text{g}^{-1}$. In this study, the term of *partition quotient* instead of
70 *partition coefficient*, is used for K_P , because *partition coefficient* is used for equilibrium
71 condition only, and ~~Equation~~Eq. (1) was not defined under equilibrium condition.

72 The value of K_P , calculated by ~~Equation~~Eq. (1) using the monitoring data TSP , C_P , and C_G ,
73 is denoted as K_{PM} (subscript “M” in K_{PM} means measurement). It has been shown that there is

74 a linear relationship between $\log K_{PM}$ and $\log K_{OA}$ (K_{OA} is Octane~~Octanol~~-air partition
75 coefficient) (Finizio et al. 1997, Harner and Bidleman, 1998, Pankow, 1998) and between
76 $\log K_{PM}$ and $\log P_L$ (P_L is sub-cooled liquid vapor pressure) (Pankow, 1987; Bidleman and
77 Foreman, 1987; Pankow and Bidleman, 1991, 1992). The $\log K_{OA}$ -based model given by

78
$$\log K_{PR} = m_O \log K_{OA} + b_O \quad (2)$$

79 has been widely used in describing the partitioning behavior for SVOCs, where slope m_O and
80 intercept b_O are fitting constants obtained using regression of $\log K_{PM}$ (from Eq. (1)) against
81 $\log K_{OA}$. The subscript “R” in K_{PR} indicates regression.

82 Unfortunately, Equation~~Eq.~~ (2) is not very useful to environmental modelers, since this
83 equation can only be used when the monitoring data of SVOCs concentrations in both gas-
84 and particle-phases are known, while the modelers need the equations to predict
85 environmental behavior, including their concentrations in air with both gaseous~~gas-~~ and
86 particulate~~particle~~-phases, based on physicochemical properties of chemicals~~SVOCs~~, their
87 emissions, climate and meteorological conditions.

88 Under the conditions of the equilibrium ($m_O=1$), the dominant absorption processes
89 between gas- and particle-phases, and equivalence of octanol to the sorbing organic matter in
90 particles, Harner and Bidleman (1998) derived the following equation,

91
$$\log K_{PE} = \log K_{OA} + \log f_{OM} - 11.91 \quad (3)$$

92 where f_{OM} is organic matter content of the particles. The subscript “E” in K_{PE} indicates
93 equilibrium. In comparison to Eq. (2), Eq. (3) has an advantage to predict K_{PE} from the values
94 of K_{OA} and f_{OM} without the need of real monitoring data.

95 However, as discussed in the previous publications (Finizio et al., 1997; Cetin and
96 Odabasi, 2007; Tian et al., 2011; Yang et al., 2013; Li and Jia, 2014), Eq. (3) cannot describe
97 accurately the relationship between gas- and particle-phases polybrominated diphenyl ethers
98 (PBDEs)~~PBDEs~~. It is evident that Eq. (3) can be applied only in a few cases, such as for less

99 brominated PBDE congeners (such as BDEs-17 and -28) or at high temperatures, and
100 becomes inaccurate in most cases, especially for highly brominated PBDE congeners, such as
101 BDE-66, -85, -99, -100, -153, -154, and -183, or at low temperatures (Yang et al., 2013; Li
102 and Jia, 2014). This has been blamed by the artifacts and nonequilibrium factors (Finizio et
103 al., 1997; Cetin and Odabasi, 2007; Tian et al., 2011; Su et al., 2006).

104 Based on a large dataset of more than 700 pairs of air samples in both gaseous-gas- and
105 particulate-particle-phases with a wide ambient temperature range of 60 °C from -22 to +38
106 °C obtained from our Chinese POPs Soil and Air Monitoring Program, Phase 2
107 (China-SAMP-II), we investigated G/P partitioning behavior of PBDEs in Chinese air (Yang
108 et al., 2013; Li and Jia, 2014). We derived for the first time empirical equations to predict the
109 values of slopes and intercepts for both K_{OA} -based and P_L -based models as functions of
110 temperature, and thus predicted partition quotient (K_P) without assuming an equilibrium
111 status and free of artifacts (Li and Jia, 2014). The slope m_O and the intercept b_O were given as
112 functions of temperature (in °C),

$$m_O(t) = 0.011t + 0.263 \quad (4)$$

$$b_O(t) = -(0.135t + 5.006) \quad (5)$$

113 The temperature t in Equation-Eqs. (4) and (5) are-is usually a mean value of temperature for
114 a series of sampling events, such as annual or monthly mean temperature at each sampling
115 site. After the values of m_O and b_O are calculated using Equation-Eqs. (4) and (5), we can use
116 Equation-Eq. (2) to calculate the values of $\log K_P$. Since this method can be used to predict the
117 values of $\log K_P$, we use K_{PP} (the second “P” in the subscript K_{PP} indicates “Prediction”)
118 instead of K_{PR} in Equation-Eq. (2), and rewrite them as
119 instead of K_{PR} in Equation-Eq. (2), and rewrite them as

$$\log K_{PP} = m_O(t) \log K_{OA} + b_O(t) \quad (6)$$

120 where $m_O(t)$ and $b_O(t)$ are given by Equations. (4) and (5), respectively.

121 It is noteworthy that $\log K_{PP}$ in Equation-Eq. (6) depends on two parameters, temperature t

124 and K_{OA} , which is also a function of temperature, and given by an empirical equation (Harner
125 and Shoeib, 2002)

126
$$\log K_{OA} = A + B/(t + 273.15) \quad (7)$$

127 where t (in $^{\circ}\text{C}$) is the temperature for each sampling event, and the parameters A and B are
128 given in **Table S1** in the Supplement for several PBDE congeners. It should be borne in mind
129 that temperature t in ~~Equations~~ (4) and (5) can be also the temperature for each sampling
130 event, and thus using ~~Equation Eq.~~ (7), we can express $\log K_{PP}$ in Equation (6) as a function of
131 a single independent variable of $\log K_{OA}$ as (Li and Jia, 2014)

132
$$\log K_{PP} (K_{OA}) = 0.011B(\log K_{OA} - 12.27)/(\log K_{OA} - A) - 2.74\log K_{OA} + 31.85 \quad (8)$$

133 These two ~~equations-Eqs.~~ (6) and (8) have been successfully applied to predict the values
134 of K_P for PBDEs as functions of $\log K_{OA}$ in air of China and other countries in the north
135 temperate zone and also at an Arctic site in East Greenland (Li and Jia, 2014), and our results
136 matched the monitoring data well at background, rural, urban, and suburban sites, but not at
137 e-waste sites due to the unpredictable PBDE emissions at these sites, and the results indicated
138 that our new equations have a better performance than ~~Equation Eq.~~ (3) in describing G/P
139 partitioning behavior of PBDEs in air as functions of $\log K_{OA}$. We also found for the first time
140 that the G/P partitioning of PBDE congeners can reach a maximum value if the ambient
141 temperature is low enough. A criterion to classify the equilibrium and nonequilibrium status
142 for PBDEs was also established using $\log K_{OA}$ (Li and Jia, 2014).

143 These equations, however, suffer from two drawbacks. First, these equations derived at the
144 temperature range from -22 to +38 $^{\circ}\text{C}$, thus cannot be used at temperatures beyond this range;
145 secondly, these equations were obtained empirically, and do not have a strong theoretical
146 foundation. Therefore, in this paper, we study the G/P partitioning behavior of PBDEs in
147 global air in a theoretical way. The objectives of this study ~~is-are~~ to establish a partitioning
148 model between gaseous and particulate phases for PBDEs, which can reveal the real

149 partitioning mechanism of PBDEs between these two phases and to predict the partition
150 quotients defined in Equation-Eq. (1) accurately for PBDEs in air, thus to achieve a
151 capability to address a series of G/P partitioning issues for these chemicals, such as those
152 presented previously (Yang et al., 2013; Li and Jia, 2014).

153

154 **2 Theory**

155 **2.1 Equilibrium state and steady state**

156 To develop a new model in simulating G/P partitioning behavior, we need to understand the
157 equilibrium state and steady state for SVOCs in environment. The steady state is a state in
158 which no change occurs with time, or all time derivatives are equal to zero. “*Equilibrium*
159 implies that phases have concentrations such that they experience no tendency for net
160 transfer of mass” (Mackay 2001). These two terms have been frequently mistaken with each
161 other. In his book (Mackay 2001), Mackay gave examples to explain the difference between
162 these two states, indicating a chemical is in equilibrium between two media (phases) as long
163 as its fugacities in the two media (phases) are equal no mater the system is steady or
164 unsteady.

165 We also noticed that, although equilibrium is actually an ideal event since such a system
166 cannot exist in real environment; this state has been successfully applied in some cases.
167 Good examples are to treat air-water exchange for gaseous pesticide
168 α -hexachlorocyclohexane (α -HCH) (Jantunen and Bidleman, 1996; 1997; Li et al. 2004) and
169 air-soil exchange for gaseous ~~ppolychlorinated biphenyls~~~~polychlorinated biphenyls~~ (PCBs)
170 (Li et al. 2010). In these two examples, the factors ~~(such as wet dissolution of gaseous~~
171 ~~α -HCH and PCBs)~~ other than the diffusion due to random molecular movement were
172 negligible, and the systems can be treated as equilibrium, thus the net flux of
173 gaseous α -HCH between air and water, and gaseous PCBs between air and soil are zero. We

realized, however, that the exchange of SVOCs between the gaseous-gas- and particulate particle-phases is different since the advection processes, such as dry and wet depositions, caused by an external force (gravity) on the particles, cannot be ignored in studying the partitioning behavior of SVOCs between these two phases. Therefore, we suggest that the steady state, not equilibrium state, should be applied here.

2.2 G/P partitioning model under steady state

2.2.1 Basic equation

A model to describe G/P partitioning under steady state for PBDEs is

$$N_{G-P} = N_{P-G} + N_{P-S} \quad (9)$$

where N_{G-P} is flux of PBDEs from gas phase to particle phase, N_{P-G} is flux of PBDEs from particle phase to gas phase, and N_{P-S} the net flux of particle-bound PBDEs between air and earth surface, such as water body or surface soil. For the sake of simplicity, we only consider dry and wet depositions in N_{P-S} , which is given by (Mackay 2001)

$$N_{P-S} = f_P (D_D + D_W) \quad (10)$$

where f_P is fugacity of particle in air, given by Eq. (S1) in the Supplement with subscript “I” being “P”, and D_D is D value of dry deposition of particle-phase PBDEs described by (Mackay 2001)

$$D_D = U_D v_P A Z_P \quad (11)$$

where U_D is dry deposition velocity, a typical value being 10 m/h, A is the area between air and earth (water or soil), and Z_P is Z value of aerosol, given by Equation-Eq. (S3) in the Supplement, and v_P is the volume fraction of aerosol, given by

$$v_P = 10^{-9} TSP / \rho \quad (12)$$

where TSP is the concentration of total suspended particles in air ($\mu\text{g}\text{-m}^{-3}$) and ρ is the density of the particle ($\text{kg}\text{-m}^{-3}$).

D_W is D value of wet deposition given by (Mackay 2001)

199 $D_W = U_R Q v_P A Z_P$ (13)

200 where U_R is rain rate, a typical value being 0.5 (m/year^{-1}). Q is a scavenging ratio
 201 representing the volume of air efficiently scavenged by rain of its particle content, per unit
 202 volume of rain. A typical value for Q of 200,000 may be used. Substituting the above 2
 203 Equations in Eq. (10) leads to

204 $N_{P-S} = f_P (U_D + U_R Q) v_P A Z_P$ (14)

205 **2.2.2 Gas/particle exchange of PBDEs**

206 One of the most important issues for investigating the G/P partitioning behavior is the
 207 exchange of PBDE between air and particles. We treat each particle as a ball with a mean
 208 diameter of d , a volume of $v = \pi d^3/6$, surface area $a = \pi d^2$, and a mass $m = \rho v$, where ρ is the
 209 density of the particle. The number of particles in 1 m^3 of air, $n = TSP/m$. In air with volume
 210 of Ah (h is the height of atmosphere), the total area of the particles is

211 $A_P = 6TSP(g/m^3) \times A(m^2)h(m)/(\rho(g/m^3)d(m))$ (15)

212 Assuming $\rho = 1.5 \times 10^6 g/m^3$, $d = 1.0 \times 10^{-7} m$ (Rissler et al. 2006), $h = 1.0 \times 10^3 m$, the above
 213 equation becomes

214 $A_P = 0.04A \times TSP$ (16)

215 To be simplified, we treat the particles as a film, called the *particle film*, with a thickness of
 216 $d = 0.1 \mu m$, a surface area of $A_P = 0.04A \times TSP \text{ m}^2$, as shown in **Fig. S1** in the Supplement. The
 217 ratio between A_P and A is

218 $R_P = A_P / A = 0.04 TSP$ (17)

219 which is a linear function of TSP .

220 In order to study the movement of SVOCs in air between air and particles, we adapted the
 221 method used for the air-soil interface introduced by Mackay (2001). For diffusion, the
 222 two-resistance approach is used, and the overall D values is given by

223 $1/D_V = 1/D_E + 1/(D_A + D_H)$ (18)

224 where D_E is air boundary layer D value, D_A and D_H are diffusion D values of chemical in air
 225 and water sub-phases in particle film, respectively. D_E is deduced as the product of the
 226 surface area of the particle film, A_P (m^2), a mass transfer coefficient k_V ($m^2/h^{1/2}$), and the Z
 227 value of air Z_G , given by:

$$228 \quad D_E = A_P k_V Z_G \quad (19)$$

229 Here,

$$230 \quad k_V = B_a / l_a \quad (20)$$

231 where B_a is the chemical's molecular diffusivity in air ($0.018 \text{ m}^2/h^{1/2}$ was assumed), and l_a is
 232 an air boundary layer thickness (0.00475 m was assumed) (Mackay 2001).

233 In comparison to the soil surface in air-soil exchange, the particle-film that we suggested
 234 in our model keeps moving within the atmosphere and thus has much more chances to
 235 intersect with the chemical in gas phase. Therefore, the mass transfer coefficient will be
 236 larger than that given by [Equation Eq. \(20\)](#), and accordingly, a [parameter fitting constant C](#) is
 237 introduced in Eq. (20), leading to

$$238 \quad k_V = C B_a / l_a \quad (21)$$

239 [Thus the term \$CB_a\$ is the chemical's molecular diffusivity for the particle film in air, and](#)
 240 [its value of C will be determined later.](#)

241 Since most of the SVOCs (including PBDEs) are associated with the organic matter of the
 242 particles, again for the sake of simplicity, the 2 terms, D_A and D_H , in Eq. (18) are neglected,
 243 which becomes

$$244 \quad D_V = D_E = A_P k_V Z_G \quad (22)$$

245 The flux of PBDEs from gas phase to particle phase, N_{G-P} , becomes

$$246 \quad N_{G-P} = f_G D_E \quad (23)$$

247 and the flux from particle phase to gas phase, N_{P-G} , is

$$248 \quad N_{P-G} = f_P D_E \quad (24)$$

249 If the term N_{P-S} is dropped from Eq. (9), i.e., the net flux of particulate-particle-bound

250 PBDEs between air and surface is neglected, we will have

251
$$N_{G-P} = N_{P-G} \quad (25)$$

252 From Eqs. (23) and (24), the fugacities of a chemical in gas-phase (f_G) and in particle
253 -phase (f_P) are equal, and thus the steady state becomes equilibrium. Therefore, it is concluded
254 that equilibrium is just a special case of steady state when N_{P-S} is ignored.

255 2.3 G/P equations under steady state

256 2.3.1 G/P partition coefficient under steady state

257 We use Eqs. (10), (23), and (24) into Eq. (9), leading to

258
$$f_P(D_E + D_D + D_W) = f_G D_E \quad (26)$$

259 By using Eqnations (S6) and (S7) in the Supplement, the above equation leads to

260
$$C'_P / C_G = (Z_P / Z_G) (D_E / (D_E + D_D + D_W)) = K_{PG} (1 / [1 + (D_D + D_W) / D_E])$$

261 where C'_P (pg/m³ of *particle*) and C_G (pg/m³ of *air*) are concentrations of SVOCs in
262 particulate-particle- and gaseous-phases, respectively, and K_{PG} is dimensionless
263 gas/particleG/P partition coefficient under equilibrium ($= Z_P / Z_G$). Setting a parameter α as

264
$$\alpha = 1 / [1 + (D_D + D_W) / D_E] \quad (27)$$

265 and the above equation becomes

266
$$C'_P / C_G = \alpha K_{PG} \quad (\text{at steady state}) \quad (28)$$

267 By using Eqnations (S10) and (S11), C'_P and K_{PG} are replaced by C_P and K_{PE} , respectively,

268 Eq. (28) becomes

269
$$(C_P / TSP) / C_G = \alpha K_{PE} \quad (29)$$

270 Defining a G/P partition coefficient under steady state,

271
$$K_{PS} = (C_P / TSP) / C_G \quad (\text{at steady state}) \quad (30)$$

272 where C_G and C_P are concentrations of PBDEs in gas- and particle-phases (both in pg m⁻³ of
273 air), respectively, *at steady state*, and the subscript “S” in K_{PS} indicates steady state. Although

274 [Equation Eq.](#) (30) seems the same as [Equation Eq.](#) (1) (for K_P) and [Equation Eq.](#) (S8) (for
 275 K_{PE}), they are different since [Equation Eq.](#) (30) is defined under steady state, [Equation Eq.](#)
 276 (S8) is under equilibrium, and [Equation Eq.](#) (1) was defined at neither steady nor equilibrium
 277 state. Thus [Equation Eq.](#) (29) becomes

278
$$\log K_{PS} = \log K_{PE} + \log \alpha \quad (31)$$

279 In the above equation, $\log K_{PE}$ is designated the *equilibrium term*, given by [Equation Eq.](#)
 280 (3), and $\log \alpha$ is the *nonequilibrium term*. Therefore, we have two predicted partition
 281 coefficients: partition coefficient K_{PS} under steady state when the system is at steady state, or
 282 partition coefficient K_{PE} under equilibrium when the system is at equilibrium. [Equation Eq.](#)
 283 (31) indicates that the equilibrium is just a special case of the steady state when $\log \alpha = 0$.

284 **2.3.2 Nonequilibrium term $\log \alpha$**

285 In [Equation Eq.](#) (27), setting

286
$$G = C (D_D + D_W) / D_E \quad (32)$$

287 [Equation Eq.](#) (27) becomes

288
$$\alpha = 1 / (1 + G/C) \quad (33a)$$

289 or

290
$$\log \alpha = -\log (1 + G/C) \quad (33b)$$

291 Substituting [Equations Eqs.](#) (11), (13) and (19) in [Equation Eq.](#) (32), which leads after some
 292 manipulations,

293
$$G = 2.09 \times 10^{-10} f_{OM} K_{OA} \quad (34)$$

294 Thus, as K_{PE} , $\log \alpha$ is also a function of f_{OM} and K_{OA} .

295 **2.4 $\log \alpha$ as functions of $\log K_{OA}$ and temperature**

296 **Fig. S2** in the Supplement depicts variation of $\log \alpha$ as functions of $\log K_{OA}$ and temperature t
 297 with $C=5$. As shown in **Fig. S2A**, the function of $\log \alpha$ versus $\log K_{OA}$ is a curve shared by all

298 PBDE congeners, showing that when $\log K_{OA} < \sim 10.4$, $\log \alpha = 0$, the state is equilibrium.

299 ~~Different from~~In contrast with – the function of $\log \alpha$ versus $\log K_{OA}$, the functions of $\log \alpha$
300 versus t are different for different PBDE congeners, as shown in **Fig. S2B** in the Supplement.
301 This figure explains why light PBDE congeners, such as BDE-17 and -28, can reach
302 equilibrium state much more easily than ~~high~~heavy PBDE congeners. It is obvious from **Fig.**
303 **S2B** that the curves of BDE-17 and -28 deviate significantly from zero at a low temperature
304 ($\sim -10^{\circ}\text{C}$), indicating that the values of $\log \alpha$ are equal or close to 0 at a wide range of
305 environmental temperature ($t > -10^{\circ}\text{C}$). For highly brominated congeners, BDE-153 for example,
306 the values of $\log \alpha$ deviates significantly from zero even when $t < +40^{\circ}\text{C}$, causing the
307 equilibrium state at a much narrower ambient temperature range for this chemical ($t > +40^{\circ}\text{C}$)
308 than BDE-17 and -28.

309 **2.5 Threshold values of $\log K_{OA}$ and temperature**

310 Since all the equations to calculate the parameter K_{PE} and K_{PS} link only the PBDE parameter
311 $\log K_{OA}$, it may be advantageous to explore partitioning behavior according to $\log K_{OA}$, rather
312 than individual PBDE congeners or homolog groups. Under this consideration, we drew
313 $\log K_{PS}$ - $\log K_{OA}$ and $\log K_{PE}$ - $\log K_{OA}$ graphs, for all PBDE congeners/homologues at an
314 environmental temperature range of -50 to $+50^{\circ}\text{C}$, as shown in **Fig. 1**. The straight line (thick
315 blue) for $\log K_{PE}$ and the curve (red) for $\log K_{PS}$ can be used for all PBDE
316 congeners/homologues as long as their ranges of $\log K_{OA}$ are known. Of course, it should be
317 mentioned that the different PBDE congeners have different ranges of $\log K_{OA}$ at the same
318 temperature span, thus are represented by different portions of the curves in the ~~Figure~~Fig. 1,
319 accordingly showing different G/P partitioning behaviors.

320 There are three cases for G in Eq. (33b).

321 (1) $G \ll C$ ($D_D + D_W \ll D_E$)

322 In this case, Eq. (33b) becomes

323 $\log \alpha = -\log (1 + G/C) \approx 0$ (35)

324 which is equilibrium state.

325 (2) $G=C$ ($D_D + D_W = D_E$)

326 In this case, Eq. (33b) becomes

327 $\log \alpha = -\log 2$ (36)

328 If we assume that $f_{OM} = 0.1$ and $C = 5$, then we have the *first threshold value* from Eqs. (33b)

329 and (34),

330 $\log K_{OA1} = 11.4$ (37)

331 which is very close to the threshold value of $\log K_{OA} = 11.5$ suggested by Li and Jia (2014). The
332 physical meaning of $\log K_{OA1}$ is, at this threshold, the data of $\log K_{PS}$ deviates from $\log K_{PE}$ by
333 an amount of $\log 2$.

334 (3) $G \gg C$ ($D_D + D_W \gg D_E$)

335 In this case, Eq. (33b) becomes

336 $\log \alpha \approx -\log (G/C) = \log C - \log K_{PE} - 2.23$ (38)

337 thus $\log K_{PS}$ in Eq. (31) reaches its maximum value,

338 $\log K_{PSM} = -1.53$ or $K_{PSM} = 0.03$ (39)

339 when $G \gg C$. This is very close to the maximum value of -1.5 suggested by Li and Jia (2014).
340 The maximum value of $\log K_{PS}$ is clearly shown in **Fig. 1** (the thin blue horizontal line), and
341 we define the *second threshold value* as

342 $\log K_{OA2} = 12.5$ (40)

343 As shown in **Fig. 1**, the first threshold value of $\log K_{OA}$ divides the whole range of $\log K_{OA}$
344 into *equilibrium* (EQ) and *nonequilibrium* *domains*—(NE) *domains*. The second threshold
345 indicates the start of the *maximum partition-domain* (MP) *domain*, in which the values of
346 $\log K_{PS}$ reach a maximum value of $\log K_{PSM}$, which is independent of the values of f_{OM} and
347 K_{OA} .

348 In brief, as shown in **Fig. 1**, the curve of $\log K_{PS}$, originally coinciding with the straight line
 349 of $\log K_{PE}$, increases along with increase of $\log K_{OA}$, and separates visibly (by a mount of $\log 2$)
 350 from the straight line of $\log K_{PE}$ at the first threshold value of $\log K_{OA1}$, entering the NE
 351 domain from the EQ domain. After the second threshold value of $\log K_{OA2}$, the curve of
 352 $\log K_{PS}$ enters the MP domain and becomes a horizontal straight line of $\log K_{PS} = -1.53$.

353 The values of $\log K_{OA}$ depend on each PBDE congener and the ambient temperature
 354 ([Harner and Shoeib, 2002](#)), as discussed previously ([Harner and Shoeib, 2002](#)). Accordingly,
 355 we defined two threshold values for temperature, the *threshold temperatures* t_{TH1} and t_{TH2} ,
 356 which are the temperatures when $\log K_{OA}$ of PBDE congeners equals to the threshold values
 357 $\log K_{OA1}$ and $\log K_{OA2}$, respectively. As presented in **Fig. 2**, while the threshold values of
 358 $\log K_{OA1}$ and $\log K_{OA2}$ are constants for all congeners, the threshold values for t_{TH1} and t_{TH2} are
 359 different for different PBDE congeners. These two threshold temperature values divided the
 360 temperature space also into the same 3 domains; the EQ domain when $t > t_{TH1}$, the NE domain
 361 when $t \leq t_{TH1} \geq t > t_{TH2}$, and the MP domain when $t \leq t_{TH2}$. Taking BDE-47 as an example, with
 362 its $t_{TH1} = +11^{\circ}\text{C}$ and $t_{TH2} = -6^{\circ}\text{C}$, BDE-47 is in EQ domain when $t > +11^{\circ}\text{C}$; in NE domain
 363 when $t \leq +11^{\circ}\text{C} \geq t > -6^{\circ}\text{C}$; and in MP domain at $t \leq -6^{\circ}\text{C}$.

364 2.6 Particle phase fraction

365 Another important parameter, the fraction of chemical on the particle phase, $\phi (=$
 366 $C_P/(C_G+C_P))$, can be calculated from K_P as

$$367 \quad \square \phi_{PX} = K_{PX} TSP / (1 + K_{PX} TSP) \quad (41)$$

368 where the subscript “PX” can be one of “PS”, “PE”, and “PR”. Thus the maximum value of
 369 particle phase fraction can be obtained from Eqs. (39) and (41) as

$$370 \quad \phi_{PSM} = 0.03 TSP / (1 + 0.03 TSP) \quad (42)$$

371 which indicates that, while the maximum partition coefficient $\log K_{PSM}$ is a constant for all
 372 PBDE congeners, its corresponding maximum value of particle phase fraction is not, but

373 depends on TSP . The variation of ϕ_{PSM} as a function of TSP is depicted in **Fig. S3** in the
374 Supplement.

375

376 **3. Application of the equations**

377 **3.1 G/P partitioning of PBDEs in Chinese Air from China-SAMP-II**

378 In the previous section, we derived an [equation-Eq.](#) (31) to predict the values of *partition*
379 *coefficient under steady state* K_{PS} . In this subsection, we used these equations to predict K_P
380 for air samples collected at 15 sites across China under our PBDE monitoring program,
381 China-SAMP-II (Yang et al., 2013, Li and Jia, 2014), and the results will be compared with
382 the predicted values of *partition coefficient under equilibrium state* K_{PE} , obtained using
383 [Equation-Eq.](#) (3); and the values of *partition quotient*, K_{PR} , obtained using [Equation-Eq.](#) (2)
384 with the help of K_{PM} , calculated from [Equation-Eq.](#) (1) using the monitoring data C_P and C_G .
385 Among the three modeled values (K_{PS} , K_{PE} , and K_{PR}), K_{PR} values are the ones most close to
386 the values of K_{PM} since $\log K_{PR}$ values are obtained directly from $\log K_{PM}$ by least squares
387 regression against $\log K_{OA}$, and the accuracy of the equations of K_{PS} and K_{PE} depends on how
388 their results close to those given by K_{PR} .

389 **Figs. S4 and S5** in the Supplement depict the variations of $\log K_{PS}$, $\log K_{PE}$, and $\log K_{PR}$ as
390 functions of $\log K_{OA}$ for the 15 sampling sites and 10 PBDE congeners, respectively, both
391 showing the curve of $\log K_{PS}$ is closer to the regression line of $\log K_{PR}$ than $\log K_{PE}$. It is
392 worthwhile to point out that, for the best match between the results of $\log K_{PS}$ and $\log K_{PR}$ for
393 PBDEs, $C = 5$ was used in Eq. (5) to calculate $\log K_{PS}$ in air at all the sampling sites with an
394 exception of the site of Waliguan, where $C = 50$ was used. The reason why much higher value
395 of C was used at this site will be explained later. **Fig. S5** also shows that, from the light
396 PBDE congeners to the heavy ones, the ranges of $\log K_{OA}$ for each PBDE congeners (at
397 temperature range of -22 °C – +38 °C) move from left to right, from smaller than $\log K_{OA1}$ for

398 BDE-17 to larger than $\log K_{\text{OA1}}$ for BDE-183, or the states that these congeners reside in
399 change from EQ domain to the NE domain, and finally reach the MP domain.

400 The 10 regression lines ($\log K_{\text{PR}}$) for the 10 PBDE congeners shown in **Fig. S5** are all
401 presented in **Fig. S6** in the Supplement along with the curves of $\log K_{\text{PE}}$ and $\log K_{\text{PS}}$, indicating
402 evidently that these 10 lines of $\log K_{\text{PR}}$ change their slopes m_0 along the curve of $\log K_{\text{PS}}$, not
403 the straight line of $\log K_{\text{PE}}$, and accordingly, the curve of $\log K_{\text{PS}}$ matches the monitored G/P
404 partitioning data very well for all the 10 PBDE congeners in Chinese air.

405 We understand that, modelers are most interested in K_{P} values as a function of temperature
406 for each PBDE congener. **Fig. S7** in the Supplement presents variations of $\log K_{\text{PS}}$, $\log K_{\text{PE}}$,
407 and $\log K_{\text{PR}}$ as functions of temperature for the 10 PBDE congeners, indicating that, the curve
408 of $\log K_{\text{PS}}$ matches the line of $\log K_{\text{PR}}$ for each PBDE congener, the highly brominated
409 congeners in particular, dramatically well. It is interesting to note that the two threshold
410 temperatures, t_{TH1} and t_{TH2} , designed by two vertical dashed lines, increase from the less
411 brominated to highly brominated PBDEs. For example, the value of t_{TH1} of BDE-17 equals to
412 -16.5°C , meaning that this compound is in the EQ domain in the most ambient temperature
413 range of $\geq -16.5^{\circ}\text{C}$, while for BDE-183, $t_{\text{TH1}}=36.5^{\circ}\text{C}$ and $t_{\text{TH2}}=15^{\circ}\text{C}$, meaning that this
414 compound is in the EQ domain only when $t > 36.5^{\circ}\text{C}$, in the NE domain when $15.0^{\circ}\text{C} < t \leq 36.5^{\circ}\text{C}$,
415 and in the MP domain when $t \leq 15.0^{\circ}\text{C}$. We also calculated the modeled values of $\log K_{\text{PS}}$
416 for 5 typical PBDE congeners as functions of temperature from -50 to $+50^{\circ}\text{C}$, and the results
417 are given in **Fig. S8** in the Supplement, showing that, along with decrease of temperature, the
418 values of $\log K_{\text{PS}}$ for PBDE congeners increase to a maximum partition value; the more highly
419 brominated the congener is, the higher is its value of the first threshold temperature (t_{TH1} , data
420 are not shown) and the second threshold temperature (t_{TH2}), and thus the higher temperatures
421 at which the congener reaches the NE and MP domains.

422 As shown in **Fig. 1**, the partitioning behavior of PBDEs depends on ambient temperature

423 of sampling events. There are three squares presented in **Fig. 1** indicating the three regions
424 with different temperature ranges, 0 $^{\circ}\text{C}$ – +50 $^{\circ}\text{C}$ (the orange one), -30 – +30 $^{\circ}\text{C}$ (the green
425 one), and -50 – 0 $^{\circ}\text{C}$ (the blue one). Here, we take the two sampling sites from
426 China-SAMP-II (Yang et al., 2013; Li and Jia, 2014), one is Harbin in the northeast of China,
427 with a sampling temperature range of -22 – +28 $^{\circ}\text{C}$, within the green square, and the other is
428 Guangzhou in the south of China, with a range of +8 – +38 $^{\circ}\text{C}$, within the orange square, as
429 examples to show how the threshold values can be used in study the G/P partitioning
430 behavior of PBDEs.

431 We determined the ranges of $\log K_{\text{OA}}$ for the 10 PBDEs at the site of Harbin (vertical bars)
432 based on the ambient temperature range of -22 – +28 $^{\circ}\text{C}$ at the site, and the results are
433 presented in **Fig. 3**. The two threshold values of $\log K_{\text{OA}}$, $\log K_{\text{OA1}}$ and $\log K_{\text{OA2}}$ (the horizontal
434 light blue dashed lines), divide the space of $\log K_{\text{OA}}$ (the left axis) into three domains, the EQ,
435 the NE, and the MP domains, and accordingly, the 10 PBDEs in Harbin air can be segregated
436 into 3 groups; BDE-17 and 28 (3-Br homologue) as equilibrium EQ-group, BDE-47 and 66
437 (4-Br homologue) as semiequilibrium SE-group, and others (>4-Br homologues) as
438 nonequilibrium NE-group. The dominant portions of $\log K_{\text{OA}}$ for the EQ-group (purple lines)
439 are under the line of $\log K_{\text{OA1}}$, i.e., these congeners are mainly in the EQ domain, while the
440 dominant or whole portions of the NE-group (blue lines) are above the line of $\log K_{\text{OA1}}$,
441 indicating that these congeners are in the NE and the MP domains. The SE-group (green lines)
442 is in both the EQ and the NE domains. It is noteworthy that, the major portions of $\log K_{\text{OA}}$ for
443 the PBDE congeners in the NE-group were in the MP domain. These three domains can also
444 be identified in the temperature space. In **Fig. 3**, the two threshold temperatures, t_{TH1} (the red
445 diamonds) and t_{TH2} (the red square), are also shown (the right axis), which is similar to **Fig. 2**.
446 In the real ambient temperature range, formed by the two red dashed lines (-22 $^{\circ}\text{C}$ and +28 $^{\circ}\text{C}$)
447 at the Harbin site, the major temperature portions of PBDEs in the EQ-group were in

448 the EQ domain ($t < t_{TH1}$), those of the NE-group in the NE and ~~the~~ MP domains ($t \geq t_{TH1}$), and
449 those of the SE-group in both the ~~both~~ EQ and ~~the~~ NE domains.

450 **Fig. 4** presents the $\log K_P$ - $\log K_{OA}$ graph for the 10 PBDEs in Harbin, which is almost
451 identical to the one contained in the green square of **Fig. 1**. The ranges of $\log K_{OA}$ for the three
452 groups and their corresponding $\log K_P$ - $\log K_{OA}$ diagram are also shown. For example, the
453 $\log K_P$ - $\log K_{OA}$ diagram for the EQ-group (3-Br homologue), bound by the 2 purple dashed
454 lines, is mainly in the EQ domain, with a small portion in the NE domain; the $\log K_P$ - $\log K_{OA}$
455 diagram for the SE group (4-Br homologue), contained by 2 green dashed lines, is mainly in
456 the NE domain, with a small portion in the MP domain; and the $\log K_P$ - $\log K_{OA}$ diagram for
457 the NE-group (>4-Br homologue), formed by the 2 blue dashed lines, is mainly in the NE and
458 ~~the~~ MP domains.

459 Similar analysis was carried out for the 10 PBDEs at the site of Guangzhou at an ambient
460 temperature range of $+8^{\circ}\text{C}$ - $+38^{\circ}\text{C}$ at the site (Yang et al., 2013), and the results are
461 presented in **Figs. S9 and S10** in the Supplement. The 10 PBDEs at Guangzhou air can also
462 be segregated into 3 groups, BDE-17, -28, and -47 as EQ-group, BDE-66, 99, and 100 as
463 SE-group, and the others, BDE-85, -99, -100, and -183 as NE-group, which are quite
464 different from those for ~~the site of~~ Harbin, caused by the different ambient temperature ranges
465 at the two sites.

466 We concluded ~~for that~~ the PBDEs in Chinese air at 15 sampling sites across China were in
467 the steady state instead of equilibrium state, in realizing that, for less brominated PBDE
468 congeners, BDE-17 and -28, this steady state can be treated as equilibrium state since their
469 nonequilibrium term ($\log \alpha$) can be ignored in comparison to the equilibrium term ($\log K_{PE}$) in
470 the temperature range of -22°C to $+38^{\circ}\text{C}$ (see **Fig. S2B**).

471

472 **3.2 G/P partitioning of PBDEs in air from other sources**

473 There are only a few data available in the literature that we can compare to our prediction
474 data.

475 We predicted the partitioning behavior of gaseous and particle-bound PBDEs in the
476 atmosphere at an e-waste site and a rural site in southern China during 2007-2008 using the
477 information given by Tian et al. (2011). We calculated the values of $\log K_{PS}$, $\log K_{PE}$, and
478 $\log K_{PR}$ as functions of $\log K_{OA}$, and the results are presented in **Fig. S11**. It is noticeable that
479 our predicted results are obviously better than those obtained by the equilibrium model at the
480 rural site, but not at the e-waste site, where the data from equilibrium model matched the
481 monitoring data better than those predicted using our equation. This seemed unexpected but
482 could possibly be explained by the fact that the emissions of PBDEs from the e-waste site
483 compensated the flux of PBDEs due to dry and wet deposition, leading a situation that
484 seemed to be at equilibrium. We cannot, however, accept the point of view that the PBDEs in
485 air at the rural area cannot reach equilibrium, but those in air at the e-waste sites can.

486 The G/P partitioning behavior was studied for 7 PBDEs (BDE-28, -47, -99, -100, -153,
487 -154 and -209) at four sites (1 suburban, 2 urban, and 1 industrial) in Izmir, Turkey, in
488 summer and winter in 2004-2005 with a temperature range of 1.8 $^{\circ}\text{C}$ – 22.4 $^{\circ}\text{C}$ (Cetin and
489 Odabasi, 2007). We calculated the particle phase PBDEs fractions ϕ_{PS} and ϕ_{PE} , using Eq. (41)
490 and compared them with the monitoring data, and the results are depicted in **Fig. S12**. It was
491 noted by the authors that their monitoring data were much lower than the predicted values by
492 the equilibrium equation (ϕ_{PE}) (Cetin and Odabasi, 2007), but it is obvious that their results
493 matched our predicted data (ϕ_{PS}) very well, among which, the best agreement was observed
494 for BDE-209, the most highly brominated congener of PBDEs.

495 We calculated the G/P partition coefficients for PBDEs in atmosphere of Kyoto, Japan,
496 which were measured in August 2000, and January and September 2001 (Hayakawa et al.,

497 2004), and the variations of $\log K_{\text{PE}}$ and $\log K_{\text{PS}}$ as functions of $\log K_{\text{OA}}$ are presented in **Fig. S13**, indicating obviously that the values of $\log K_{\text{PS}}$ was in a better agreement with the monitoring data than $\log K_{\text{PE}}$.

500 Air samples were collected from 1 urban, 2 rural, and 1 remote sites near the Great Lakes
501 in 1997-1999 as part of the Integrated Atmospheric Deposition Network (IADN), among
502 which, those taken when the ambient atmospheric temperatures were 20 ± 3 °C were
503 analyzed for the G/P partitioning behavior of PBDEs, and the log-log relation of K_{P} and their
504 subcooled liquid vapor pressures (P_{L}) for BDE-47, -99, -100, -153, and -154 were calculated
505 (Strandberg et al. 2001). By using these data, we calculated both $\log K_{\text{P}}$ and ϕ_{P} as functions of
506 $\log K_{\text{OA}}$ for the same 5 PBDE congeners, using the values of $f_{\text{OM}} = 0.2$ and $TSP = 25 \mu\text{g m}^{-3}$
507 suggested by Harner and Shoeib (2002), which are presented in **Fig. S14**, along with the
508 predicted results under equilibrium state and steady state. Again the results indicated that the
509 prediction by our new equation is more accurate than those by the equilibrium equation.

510 **3.3 G/P partitioning of PBDEs in the Arctic air**

511 As discussed in the previous sections, each PBDE congener will reach the maximum partition
512 domain when $\log K_{\text{OA}} \geq \log K_{\text{OA}2}$ or $t \leq t_{\text{TH2}}$. The value of t_{TH2} of BDE-183 is 15 °C, meaning
513 that BDE-183 in air will be in MP domain when $t < 15$ °C. The value of t_{TH2} for BDE-209
514 should be higher ($\log K_{\text{OA}} = 14.98$ for BDE-209 was estimated at 25 °C by Cetin and Odabasi
515 (2007) in comparison to $\log K_{\text{OA}} = 11.97$ for BDE-183 at the same temperature). Accordingly,
516 BDE-209 in ~~the~~ arctic air should be in the MP domain, with a constant of $\log K_{\text{PSM}} (= -1.53)$
517 and the corresponding $\phi_{\text{PSM}} (= 0.23$ if $TSP = 10 \mu\text{g m}^{-3}$ is assumed). This prediction was
518 remarkably in agreement with monitoring data for BDE-209 measured in arctic air at Alert,
519 Canada from 2007 to 2009 with a temperature range between 10 and -50 °C (NCP 2013),
520 lower than the value of t_{TH2} for BDE-209 (see **Fig. 5**). The comparisons between the
521 predicted values and the monitoring data at Alert for other values of $TSP (= 5$ and $2 \mu\text{g m}^{-3}$)

522 given in **Fig. S15** also showed great consistence. It should be stressed from the figure that the
523 values of $\log K_{\text{PE}}$ of BDE-209 are from 3.06 at 10 °C to 8.36 at -50 °C calculated by Eq. (3),
524 which means that the values of K_{PE} are from more than 5 orders at 10 °C to 10 orders at -50
525 °C of magnitude higher than the monitoring data, a huge error that cannot be tolerated. The
526 corresponding values of ϕ_{PE} are 1, indicating that BDE-209 are all in particle phase in the
527 Arctic air predicted by the equilibrium equation, which was not the case given by the
528 monitoring data. In other words, the maximum value 0.23 of ϕ_{PSIPSM} indicates that, from our
529 prediction, more than half BDE-209 (~0.77) is in gas phase in the Arctic air, which was
530 confirmed by the monitoring data shown in **Fig. 5**.

531 We also studied the G/P partition for the 10 PBDEs (BDE-28, -47, -66, -85, -99,
532 -100, -153, -154, -183, and -209) in the Arctic atmosphere in East Greenland Sea in
533 August and September 2009 with a temperature range between -0.5 °C and +6.5 °C (Möller et
534 al., 2011). We calculated the values of $\log K_{\text{PS}}$, $\log K_{\text{PE}}$, and $\log K_{\text{PR}}$ as functions of $\log K_{\text{OA}}$,
535 and the results are shown in **Fig. S16**. Once again, the equation of $\log K_{\text{PS}}$ had a better
536 performance than the equation of $\log K_{\text{PE}}$, especially for those congeners in the NE domain
537 with $\log K_{\text{OA}} \geq \log K_{\text{OA1}}$.

538

539 **4. Conclusions and Discussions**

540 **4.1 G/P partitioning of PBDEs in global air**

541 **Figure At a Glance** in the Supplement presents G/P partition coefficients of PBDEs ($\log K_{\text{PS}}$
542 and $\log K_{\text{PE}}$) as functions of $\log K_{\text{OA}}$ at ambient temperature ranging from -50 °C to +50 °C,
543 which can be applied at any sites worldwide (the top middle panel, similar to **Fig. 1**). The
544 three squares in the panel designate the $\log K_{\text{P}}\text{-}\log K_{\text{OA}}$ graphs with three different temperature
545 ranges: 0 °C – +50 °C, -30 °C – +30 °C, and -50 °C – 0 °C, representing the tropical and
546 subtropical climate zones, warm temperate climate zone, and boreal and tundra climate zones,

547 respectively. Monitoring data ($\log K_{PM}$), their regression data ($\log K_{PR}$), and the predicted
548 results $\log K_{PS}$ and $\log K_{PE}$ in the three different temperature zones are presented in the figure;
549 the site Guangzhou, China, within the subtropical climate zone, shown in the top-left panel,
550 the site Harbin, China, within the warm temperate climate zone, shown in the bottom panel,
551 and in the site Alert, Canada, within tundra climate zone, shown in the top-right panel, all
552 introduced in the previous sections. The data at these three sampling sites all indicated that
553 the curve of our new equation ($\log K_{PS}$) are superior to the equilibrium equation ($\log K_{PE}$) in
554 G/P prediction of partitioning behavior for PBDEs in global air, at the sites in warm
555 temperate, boreal, and tundra climate zones.

556 **4.2 Equilibrium state vs steady state**

557 Harner and Bidleman (1998) developed in 1998 the [equation-Eq.](#) (3), which can predict
558 for the first time the partition coefficients of selected SVOCs in air under the condition of
559 equilibrium between gas- and particle-phases. Four years later, Harner and Shoeib (2002)
560 used this equation to predict the partitioning behavior for 11 PBDE congeners at 25 °C and 0
561 °C, the results of which, along with the results from our new equation under steady state, are
562 given in **Fig. S17** in the Supplement. As shown in the figure, the equilibrium [equation-Eq.](#) (3)
563 predicted that, at 0 °C, the particle fraction of PBDE congeners can reach as high as ~1,
564 which means that PBDE congeners can completely sorbed to the particles. According to our
565 new [equation-Eq.](#) (31) under steady state, however, the maximum particle fraction of PBDE
566 congeners was about 0.42 when $\log K_{OA} \geq \log K_{OA2}$, which was less than half of the highest
567 values predicted by [Equation-Eq.](#) (3). In other words, we predict that the maximum particle
568 fraction of PBDE congeners in air cannot be more than 50% under steady state if $TSP < 30$
569 $\mu\text{g}/\text{m}^3$ (See **Fig. S3** in the Supplement). In order to support their prediction results, Harner
570 and Shoeib (2002) used the monitoring data of gaseous and [particulate particle-bound](#) PBDEs
571 in the Great Lakes air at 20 ± 3 °C (Strandberg et al. 2001). However, as demonstrated in **Fig.**

572 **S14**, the prediction by our new equation is much accurate than those by the equilibrium
573 equation. This suggests that PBDEs in the Great Lakes atmosphere were in the steady state,
574 not in the equilibrium state.

575 In brief, we cannot treat the gas- and particle-phases as a closed system for studying
576 ~~gas/particleG/P~~ partitioning behavior of PBDEs, since the third compartment, the surface of
577 the earth has to be considered. If the nonequilibrium term, $\log\alpha$, in ~~Equation-Eq.~~ (31) cannot
578 be ignored, then the fugacities of PBDEs in gas- and particle-phases are not equal, indicating
579 that the system is not at equilibrium but at steady state. For some ~~low-less~~ brominated PBDEs
580 (such as BDE-17 and -28) at certain temperature, the values of $\log\alpha$ is small enough in
581 comparison to the value of $\log K_{PE}$ in Eq. (31), which is considered as a small perturbation,
582 the system can be considered as equilibrium.

583 **4.3 The maximum partition coefficient**

584 In our previous study (Li and Jia, 2014), we predicted for the first time by an empirical
585 approach the existence of a maximum partition coefficient that every PBDE congener can
586 reach, and was wrongly termed as “saturation state”. This prediction was confirmed in this
587 study by a theoretical approach. As shown in **Fig. 1**, the logarithm of the maximum partition
588 coefficient $\log K_{PSM}$ is equal to -1.53 (or $K_{PSM} = 0.03$) when $\log K_{OA} \geq \log K_{OA2}$ ($=12.5$ for all
589 PBDE congeners), or equally when the ambient temperature is smaller than or equal to t_{TH2} ,
590 which is from -34.5 °C for BDE-17 to 15 °C for BDE-183, and cannot increase linearly along
591 with increase of $\log K_{OA}$ as predicted by the straight line of $\log K_{PE}$. The difference of
592 prediction data between these two equations can be very great. For example, as shown in **Fig.**
593 **1**, the difference can reach as high as ~5.5 order of magnitude when $\log K_{OA} = 17$. Obviously,
594 the state in the MP domain is a steady state, but not an equilibrium state since the fugacities
595 of PBDEs in gas- and particle-phases are not equal.

596 The best example is the case for BDE-209 in the Canadian ~~arctic-Arctic~~ site Alert predicted

597 by our new steady equation discussed previously (**Fig. 5**). In fact, this is true for any PBDE
598 congener, not for BDE-209 only. As shown in **Fig. 1**, the blue square with a temperature
599 range of -50 $^{\circ}\text{C}$ – 0 $^{\circ}\text{C}$ could most likely be the situation for the Arctic atmosphere. **Fig. 2**
600 shows that, for the 7 PBDE congeners (BDE-66, -85, -99, -100, 153, -154, and -183), $t_{\text{TH2}} > 0$
601 $^{\circ}\text{C}$. Thus we predict that, as the G/P partitioning behavior is considered, these 7 PBDE
602 congeners do not behave differently in the Arctic air, and are all have the same partition
603 coefficient, $\log K_{\text{PSM}} = -1.53$. Unfortunately, there are no data for the PBDE congeners other
604 than BDE-209 available for confirmation of this prediction in the Arctic air.

605 **4.4 Comparison to the empirical equations**

606 The two empirical ~~equations-Eqs.~~ (6) and (8) have been successfully applied to predict the
607 values of K_{P} for PBDEs in air of China and other countries in the north temperate zone and
608 also at an Arctic site in East Greenland (Li and Jia, 2014). The ~~steady-equationEq.~~ (31) for
609 $\log K_{\text{PS}}$ derived in this study is superior to these empirical equations $\log K_{\text{PP}}$ and $\log K_{\text{PP}}(K_{\text{OA}})$
610 in two ways. First, the steady-state ~~equation-Eq.~~ (31) was derived theoretically, and secondly,
611 this ~~steady-steady-state~~ equation can be used at any ambient temperature, from equator to
612 polar regions, while the empirical equations can only be used at a temperature range of -22 $^{\circ}\text{C}$
613 to +38 $^{\circ}\text{C}$.

614 Comparison between ~~steady-steady-state equation-Eq.~~ (31) for $\log K_{\text{PS}}$ and empirical
615 equations $\log K_{\text{PP}}$ given by Eq. (6) and $\log K_{\text{PP}}(K_{\text{OA}})$ given by Eq. (8) in Harbin air at a
616 temperature range of -22 to +28 $^{\circ}\text{C}$ are presented in **Fig. 6**, and the equilibrium equation
617 $\log K_{\text{PE}}$, given by Eq. (3), is also included for comparison. It is evident from **Fig. 6** that, the
618 straight line $\log K_{\text{PP}}$ deviates apparently from the straight line $\log K_{\text{PE}}$ at $\log K_{\text{OA}} = \log K_{\text{OAI}}$,
619 and increases linearly with $\log K_{\text{OA}}$. Different lines of $\log K_{\text{PP}}(K_{\text{OA}})$ for different PBDE
620 congeners are able to predict the G/P partitioning behavior of PBDE more accurately than the
621 straight line $\log K_{\text{PP}}$. It is interesting to note that, the different lines of $\log K_{\text{PP}}(K_{\text{OA}})$ for

622 different PBDE congeners change their trends along with the single line of ~~steady~~
623 ~~steady-state~~ equation $\log K_{PS}$, which is the best equation that can be used to predict the G/P
624 partitioning ~~behaviour~~~~behavior~~ for all PBDE ~~compounds~~~~congeners~~ and at all ranges of
625 ambient temperature.

626 **4.5 The limitation of applications**

627 In order to derive Eq. (31), several assumptions were made, which include that, the G/P
628 partitioning reached steady state, the annual rainfall was 0.5 m yr^{-1} , $f_{OM} = 0.1$, $C = 5$, and
629 some others. This equation, however, has been ~~able to be~~ successfully applied in all situations
630 that we discussed in this study, in which some of the assumptions were not satisfied. We
631 should be aware, however, that the situations in which some abnormal conditions exist, such
632 as heavy wind, heavy rains, or the sampling sites close to e-waste or PBDE manufactures,
633 should be best treated separately. For example, as described in the previous section, the
634 constant C should be changed from 5 to 50 in Eq. (5) for Site Waliguan. The reason why
635 much higher value of C was used at this site is possibly due to the high wind speed there. At
636 Waliguan, where annual average wind speed reaches 4.6 m/s, and the northwest wind with
637 speed $> 10 \text{ m/s}$ being quite often in the winter and spring seasons
638 (<http://gaw.empa.ch/gawsis/reports.asp?StationID=12>), much higher than the other sites; and
639 the air sampler was installed at the top of the mountain (see Supplementary Fig. S18),
640 suffering from the highest wind speed without any blocks in the area, causing the higher
641 value of C than those at the other 14 sites. An analytic equation may exist to relate the
642 parameter C and the wind speed (and possibly other factors too), but this equation is not
643 available at present and ~~planned~~ for ~~a~~ future study. The case for the Chinese e-waste site is
644 also worth to mention. Our equation cannot be used at the e-waste sites and most likely at the
645 PBDE manufacturers as well since the emissions of PBDEs at these sites could be too large
646 and also variable with time so that the steady state cannot be reached or maintained

647 It should be borne in mind that the steady state discussed here is still an idealized scenario
648 since only dry and wet depositions were discussed in the study, other factors, such as
649 humidity and artifacts, will also play roles to a certain extent to affect the G/P partitioning.As
650 equilibrium is an idealized scenario not presenting in real environment, the steady state
651 discussed here is also an ideal one, since only dry and wet depositions were discussed. As
652 anticipated, results obtained from this study do not perfectly fit monitoring data. However,
653 this study revealed the major internal factors governing the gas-particle partitioning processes
654 for PBDEs, and explicated how these processes can be more correctly treated as being in
655 steady state rather than in equilibrium state. At least, the steady steady-state model, not the
656 equilibrium-state model, should be applied to analyze the gas-particle relationship of SVOCs,
657 such as PBDEs. Further study for other SVOCs, like PCBs and PAHs, is on the way.

658

659 **The Supplement related to this article is available online at**

660

661 **Author contribution:**

662 Y.F.L. designed the research on the new theory of G/P partitioning of PBDE in air under
663 steady state; Y.F.L., W.L.M., and M.Y. performed the research; Y.F.L., W.L.M, and M.Y.
664 analyzed data; and Y.F.L. wrote the paper, with input from W.L.M., and M.Y.

665

666

667 **Acknowledgment**

668 This work was supported by the Fundamental Research Funds for the Central Universities
669 (Grant No. HIT.KISTP.201427) and the National Natural Science Foundation of China (No.
670 21277038). The authors thank IJRC-PTS colleagues and students for their contributions to
671 the China POPs SAMP-II. Valuable comments and editorial work from K. Kannan from

672 Wadsworth Center, New York State Department of Health, and Department of Environmental
673 Health Sciences, School of Public Health, State University of New York at Albany, J. Li from
674 Stanford University, M. Alaee from Environment Canada, and Y. Su from Ontario Ministry of
675 Environment, Canada, are highly appreciated. Thanks are also to D. Mackay of Trent
676 University, Canada, for his encouragement and valuable comments when Y.F. Li (one of the
677 coauthors) presented this work to Mackay's group.

678

679 **References**

680 Barrie, L. A., Gregor, D., Hargrave, B., Lake, R., Muir, D., Shearer, R., Tracey, B., and
681 Bidleman, T.: Arctic contaminants: sources, occurrence and pathways. *Sci. Total Environ.*,
682 122, 1-74, 1992.

683 Bidleman, T. F.: Atmospheric processes. *Environ. Sci. Technol.*, 22, 361-367, 1988.

684 Bidleman, T. F. and Harner, T.: Sorption to Aerosols, in *Handbook of Property Estimation
685 Methods for Chemicals: Environmental and Health Sciences*. (eds Boethling, R.S. and
686 Mackay, D.), Lewis Publishers, Boca Raton, FL. 2000.

687 Bidleman, T. F., and Foreman, W. T.: 1987. Vapor-particle partitioning of semivolatile organic
688 compounds. In *Sources and Fates of Aquatic Pollutants*, ed. R. A. Hites and S. J.
689 Eisenreich, pp. 29-56. American Chemical Sot., Washington, District of Columbia.

690 Cetin, B. and Odabasi, M.: Atmospheric concentrations and phase partitioning of
691 polybrominated diphenyl ethers (PBDEs) in Izmir, Turkey. *Chemosphere* 71, 1067-1078,
692 2007.

693 Eckhardt, S. K. B. and Manø, S. S. A.: Record high peaks in PCB concentrations in the Arctic
694 atmosphere due to long-range transport of biomass burning emissions. *Atmos. Chem.
695 Phys.*, 7, 4527-4536, 2007.

696 Finizio, A., Mackay, D., Bidleman, T. F., Harner, T.: Octanol-air partition coefficient as a
697 predictor of partitioning of semi-volatile organic chemicals to aerosols. *Atmos. Environ.*,
698 15: 2289-2296, 1997.

699 Halsall, C. J. L., Barrie, A., Fellin, P., Muir, D.C.G., Billeck, B.N., Lockhart, L., Rovinsky, F.
700 Ya., Kononov, E.Ya., and Pastukhov, B.: Spatial and temporal variation of polycyclic
701 aromatic hydrocarbons in the Arctic atmosphere. *Environ. Sci. Technol.*, 31, 3593-3599,
702 1997.

703 Harner, T. and Bidleman, T. F.: Octanol-air partition coefficient for describing particle/gas

704 partitioning of aromatic compounds in urban air. Environ. Sci. Technol., 32, 1494-1502,
705 1998.

706 Harner, T. and Shoeib, M.: Measurements of octanol-air partition coefficients (K_{OA}) for
707 polybrominated diphenyl ethers (PBDEs): Predicting partitioning in the environment. J.
708 Chem. Eng. Data, 47, 228-232, 2002.

709 Hayakawa K, Takatsuki H, Watanabe I, Sakai S.: Polybrominated diphenyl ethers (PBDEs),
710 polybrominated dibenzo-p-dioxins/dibenzofurans (PBDD/Fs) and
711 monobromo-polychlorinated dibenzo-p-dioxins/dibenzofurans (MoBPXDD/Fs) in the
712 atmosphere and bulk deposition in Kyoto, Japan. Chemosphere, 57, 343-356, 2004.

713 Helm, P. A. and Bidleman, T. F.: Gas-particle partitioning of polychlorinated naphthalenes
714 and non- and mono-ortho-substituted polychlorinated biphenyls in arctic air. Sci. Total.
715 Environ., 342, 161-173, 2005.

716 Hung, H., Blanchard, P., Poole, G., Thibert, B., Chiu, C. H.: Measurement of
717 particle-bound polychlorinated dibenzo-p-dioxins and dibenzofurans (PCDD/Fs) in Arctic
718 air at Alert, Nunavut, Canada. Atmos. Environ., 36, 1041-1050, 2002.

719 Jantunen, L. M. and Bidleman, T.: Air-water gas exchange of hexachlorocyclohexanes
720 (HCHs) and the enantiomers of α -HCH in Arctic regions. J. Geophys. Res., 101,
721 28837-28846, 1996.

722 Jantunen, L. M. and Bidleman, T.: Correction to "Air-water gas exchange of
723 hexachlorocyclohexanes (HCHs) and the enantiomers of α -HCH in arctic regions" by
724 Liisa M Jantunen and Terry Bidleman. J. Geophys. Res., 102, 19279-19282, 1997.

725 Li Y. F. and Jia, H. L.: Prediction of Gas/Particle Partition Quotients of Polybrominated
726 Diphenyl Ethers (PBDEs) in north temperate zone air: An empirical approach, Ecotoxic.
727 Environ. Safety, 108, 65-71, 2014.

728 Li, Y. F., Bidleman, T. F., Barrie, L. A., and McConnell, L. L.: Global hexachlorocyclohexane

729 use trends and their impact on the arctic atmospheric environment. *Geophys. Res. Lett.*,
730 25, 39-41, 1998.

731 Li, Y. F. and Bidleman, T. F.: Correlation between global emissions of
732 α -hexachlorocyclohexane and its concentrations in the Arctic Air. *J. Environ. Inform.*, 1,
733 52-57, 2003.

734 Li, Y. F., Macdonald, R. W., Ma, J., Hung, H., Venkatesh, S., α -HCH Budget in the Arctic
735 Ocean: The Arctic Mass Balance Box Model (AMBBM), *Sci. Total. Environ.*, 324,
736 115-139, 2004.

737 Li, Y. F., Harner, T., Liu, L., Zhang, Z., Ren, N. Q., Jia, H., Ma, J., Sverko, E.:
738 Polychlorinated biphenyls in global air and surface soil: Distributions, air - soil exchange,
739 and fractionation effect. *Environ. Sci. Technol.*, 44, 2784-2790, 2010.

740 Lohmann, R., Harner, T., Thomas, G. O. and Jones, K.C.: A comparative study of the
741 gas-particle partitioning of PCDD/Fs, PCBs and PAHs. *Sci. Total. Environ.*, 34,
742 4943-4951, 2000.

743 Macdonald, R. W., Barrie, L. A., Bidleman, T. F., Diamond, M. L., Gregor, D. J., Semkin, R.
744 G., Strachan, W. M., Li, Y. F., Wania, F., Alaee, M., Alexeeva, L. B., Backus, S. M., Bailey,
745 R., Bewers, J. M., Gobeil, C., Halsall, C. J., Harner, T., Hoff, J. T., Jantunen, L. M.,
746 Lockhart, W. L., Mackay, D., Muir, D. C., Pudykiewicz, J., Reimer, K. J., Smith, J. N.,
747 Stern, G. A.: Contaminants in the Canadian Arctic: 5 years of progress in understanding
748 sources, occurrence and pathways. *Sci. Total. Environ.*, 254, 93-234, 2000.

749 Mackay, D. 2001. *Multimedia Environmental Models: The Fugacity Approach*, 2nd Edition,
750 Taylor & Francis, New York. p: 261.

751 M öller, A, Xie, Z, Sturm R, and Ebinghaus, R.: Polybrominated diphenyl ethers (PBDEs) and
752 alternative brominated flame retardants in air and seawater of the European Arctic.
753 *Environ. Pollut.*, 159, 1577-1583, 2011.

754 NCP 2013: Canadian Arctic Contaminants Assessment Report On Persistent Organic
755 Pollutants – 2013 (eds Muir D, Kurt-Karakus P, Stow J.). (Northern Contaminants
756 Program, Aboriginal Affairs and Northern Development Canada, Ottawa ON. xxiii + 487
757 pp + Annex 2013.

758 Pankow, J. F.: An absorption model of gas/particle partitioning in the atmosphere. *Atmos.*
759 *Environ.*, 28, 185-188, 1994.

760 Pankow, J. F.: Interdependence of the slopes and intercepts from log-log correlations of
761 measured gas-particle partitioning and vapor pressure—I. theory and analysis of available
762 data. *Atmos. Environ.*, 26A, 1071-1080, 1992.

763 Pankow, J.F.: Review and comparative analysis of the theories on partitioning between the
764 gas and aerosol particulate phases in the atmosphere. *Atmos. Environ.*, 21, 2275-2283,
765 1987.

766 Pankow, J.F.: Further discussion of the octanol/air partition coefficient K_{oa} as a correlating
767 parameter for gas/particle partitioning coefficients. *Atmos. Environ.* 32, 1493-1497, 1998.

768 Pankow, J. F., and Bidleman, T. F.: Effects of temperature, TSP and percent
769 non-exchangeable material in determining the gas-particle partitioning of organic
770 compounds. *Atmos. Environ.*, 25A, 2241-2249, 1991.

771 Pankow, J. F., and Bidleman, T. F.: Interdependence of the slopes and intercepts from log-log
772 correlations of measured gas-particle partitioning and vapor pressure-I. Theory and
773 analysis of available data. *Atmos. Environ.*, 26A, 1071-1080, 1992.

774 Rissler, J., Vestin, A., Swietlicki, E., Fisch, G., Zhou, J., Artaxo, P., and Andreae, M.O.: Size
775 distribution and hygroscopic properties of aerosol particles from dry-season biomass
776 burning in Amazonia. *Atmos. Chem. Phys.*, 6, 471-491, 2006.

777 Strandberg, B., Dodder, N. G., Basu, I., and Hites, R. A.: Concentrations and spatial
778 variations of polybrominated diphenyl ethers and other organohalogen compounds in

779 Great Lakes air. Environ. Sci. Technol., 35, 1078-1083, 2001.

780 Su, Y., Lei, Y. D., Wania, F., Shoeib, M., Harner, T.: Regressing gas/particle partitioning
781 data for polycyclic aromatic hydrocarbons. Environ. Sci. Technol., 40, 3558-3564, 2006.

782 Tian, M., Chen, S., Wang, J., Zheng, X., Luo, X., and Mai, B.: Brominated flame retardants
783 in the atmosphere of e-waste and rural sites in Southern China: Seasonal
784 variation, temperature dependence, and gas-particle partitioning. Environ. Sci.
785 Technol., 45, 8819-8825, 2011.

786 Weschler, C. J. and Nazaroff, W.W.: Semivolatile organic compounds in indoor environments.
787 Atmos. Environ., 42, 9018-9040, 2008.

788 Weschler, C. J.: Indoor/outdoor connections exemplified by processes that depend on an
789 organic compound's saturation vapor pressure. Atmos. Environ., 37, 5455-5465, 2003.

790 Yamasaki, H., Kuwata, K., and Miyamoto, H.: Effects of ambient temperature on aspects of
791 airborne polycyclic aromatic. Environ. Sci. Technol., 16, 189-194, 1982.

792 Yang, M., Qi, H., Jia, H., Ren, N., Ding, Y., Ma, W., Liu, L., Hung, H., Sverko, E., and Li, Y.
793 F.: Polybrominated diphenyl ethers (PBDEs) in air across China: Levels, compositions,
794 and gas-particle partitioning. Environ. Sci. Technol., 47, 8978-8984, 2013.

795

796

797 **Figure captions**

798 **Figure 1.** Variation of $\log K_{\text{PE}}$ and $\log K_{\text{PS}}$ as functions of $\log K_{\text{OA}}$ with a temperature range of
799 -50°C – $+50^{\circ}\text{C}$. Two threshold values of $\log K_{\text{OA}}$ ($\log K_{\text{OA}1}$ and $\log K_{\text{OA}2}$) are also shown,
800 which divide the space of $\log K_{\text{OA}}$ into three domains: the equilibrium (EQ), the
801 nonequilibrium (NE), and the maximum partition (MP) domains. The three squares
802 designate the $\log K_{\text{P}}$ - $\log K_{\text{OA}}$ graphs with three different temperature ranges: 0°C – $+50^{\circ}\text{C}$,
803 -30°C – $+30^{\circ}\text{C}$, and -50°C – 0°C , representing the tropical and subtropical climate
804 zones, warm temperate climate zone, and boreal and tundra climate zones, respectively.

805 **Figure 2.** The first and second threshold temperatures, t_{TH1} and t_{TH2} for 10 PBDE congeners,
806 which divide the temperature space into the same 3 domains (EQ, NE, and MP).

807 **Figure 3.** The range of $\log K_{\text{OA}}$ (the left axis) and the threshold temperatures (the right axis)
808 for 10 PBDE congeners in Harbin air at a temperature range of -22 to $+28^{\circ}\text{C}$. The
809 ranges of $\log K_{\text{OA}}$ for the 10 PBDE congeners are given by the vertical bars. The 2
810 horizontal light blue dashed lines give the 2 threshold values of $\log K_{\text{OA}1}$ and $\log K_{\text{OA}2}$,
811 and the red diamonds and red squares present respectively the two corresponding
812 threshold temperatures, t_{TH1} and t_{TH2} . The former divides the space of $\log K_{\text{OA}}$ (the left
813 axis) and the later divides the temperature space (the right axis) into three domains: the
814 EQ domain, the NE domain, and the MP domain. Thus the PBDE congeners
815 (homologues) in Harbin air can be segregated into 3 groups; BDE-17 and -28 (3-Br
816 homologue) as equilibrium EQ-group, BDE-47 and -66 (4-Br homologue) as
817 semiequilibrium SE-group, and others (>4 -Br homologues) as nonequilibrium
818 NE-group.

819 **Figure 4.** The $\log K_{\text{P}}$ - $\log K_{\text{OA}}$ diagram for the 10 PBDE congeners in Harbin air at a
820 temperature range of -22 to $+28^{\circ}\text{C}$. The EQ Group includes BDE-17 and -28 , the SE
821 Group contains BDE-47 and -66 , and the rests belong to NQ Group. The range of

822 $\log K_{OA}$ for each group and their corresponding $\log K_P$ - $\log K_{OA}$ diagram are also shown.
823 The $\log K_P$ - $\log K_{OA}$ diagram for the EQ Group, bounded by 2 purple dashed lines, is
824 mainly in the EQ domain, with a small portion in NE domain; the $\log K_P$ - $\log K_{OA}$
825 diagram for the SE Group, contained by 2 green dashed lines, is mainly in the NE
826 domain, with a small portion in MP domain; and the $\log K_P$ - $\log K_{OA}$ diagram for the NE
827 Group, formed by the 2 blue dashed lines, is mainly in the NE and MP domains.

828 **Figure 5.** The temporal trends of concentrations of BDE-209 in the Arctic air in gas + particle
829 phase (blue line) and in particle phase (green line) at Alert, Canada from 2007 to 2009
830 (NCP 2013). The purple triangles and red diamonds are the values of ϕ and $\log K_P$ of
831 BDE-209, respectively, calculated using the concentration data, and match well the
832 values of ϕ_{PSM} ($=0.23$) and $\log K_{PSM}$ (-1.53), respectively ($TSP = 10 \mu\text{g m}^{-3}$ was
833 assumed).

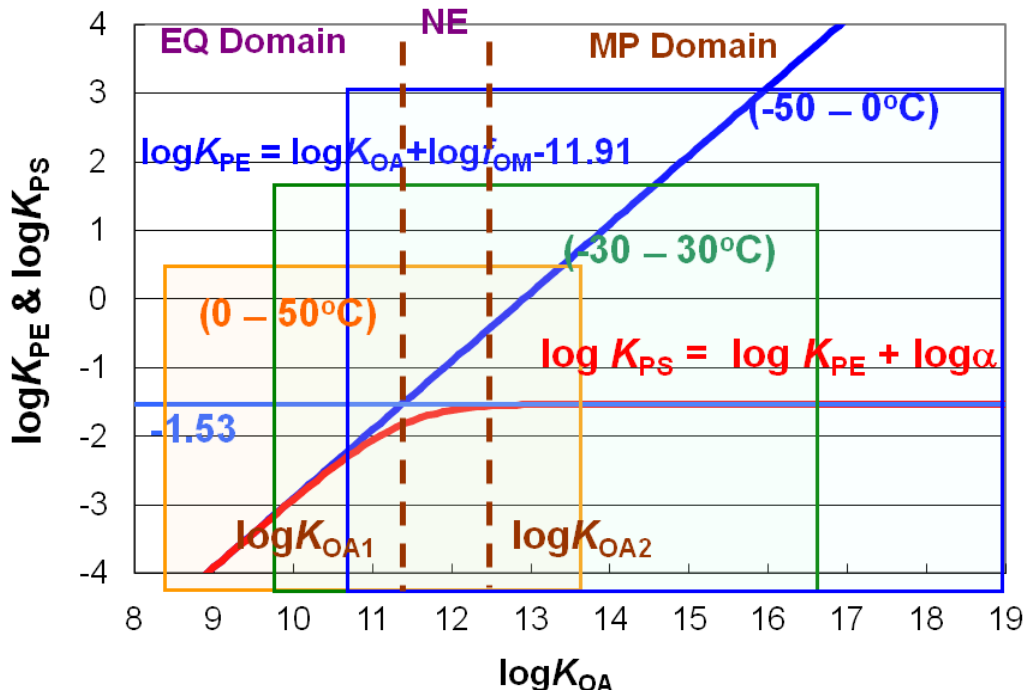
834 **Figure 6.** Variation of $\log K_{PS}$ (the thick red line, given by Eq. (31)), $\log K_{PE}$ (the thick dark
835 green line, given by Eq. (3)), and $\log K_{PP}$ (the thick pink line, given by Eq. (6)) as
836 functions of $\log K_{OA}$. The functions of $\log K_{PP}(K_{OA})$ (the thin lines, given by Eq. (8))
837 versus $\log K_{OA}$ for the 10 PBDE congeners in Harbin air at a temperature range of -22 to
838 $+28^{\circ}\text{C}$ are also included.

839
840

841

842 **Figures**

843

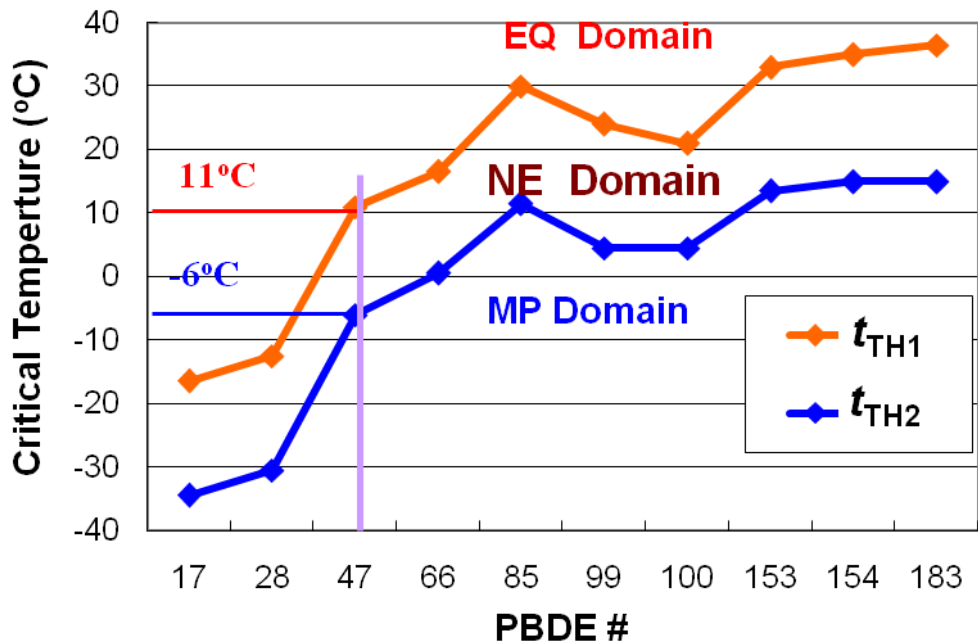


844

845 **Figure 1.** Variation of $\log K_{PE}$ and $\log K_{PS}$ as functions of $\log K_{OA}$ with a temperature range of
 846 $-50^{\circ}\text{C} - +50^{\circ}\text{C}$. Two threshold values of $\log K_{OA}$ ($\log K_{OA1}$ and $\log K_{OA2}$) are also shown,
 847 which divide the space of $\log K_{OA}$ into three domains: the equilibrium (EQ), the
 848 nonequilibrium (NE), and the maximum partition (MP) domains. The three squares designate
 849 the $\log K_{P}$ - $\log K_{OA}$ graphs with three different temperature ranges: $0 - +50^{\circ}\text{C}$, $-30 - +30^{\circ}\text{C}$,
 850 an $-50 - 0^{\circ}\text{C}$, representing the tropical and subtropical climate zones, warm temperate
 851 climate zone, and boreal and tundra climate zones, respectively.

852

853

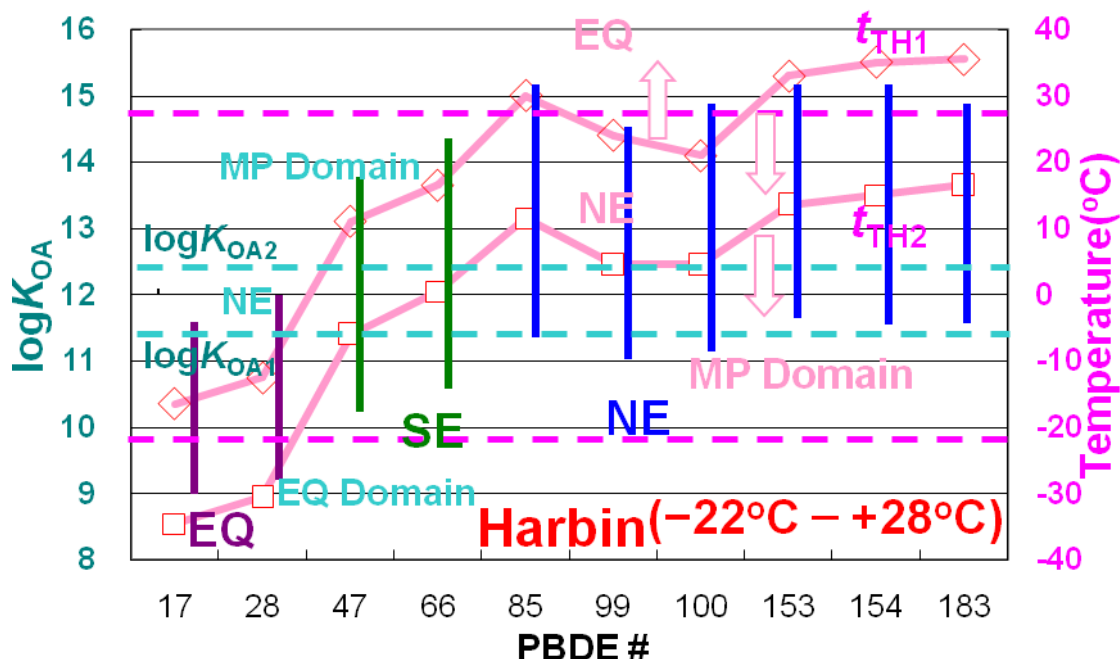


854

855 **Figure 2.** The first and second threshold temperatures, t_{TH1} and t_{TH2} for 10 PBDE congeners,
 856 which divide the temperature space into the same 3 domains (EQ, NE, and MP).

857

858



859

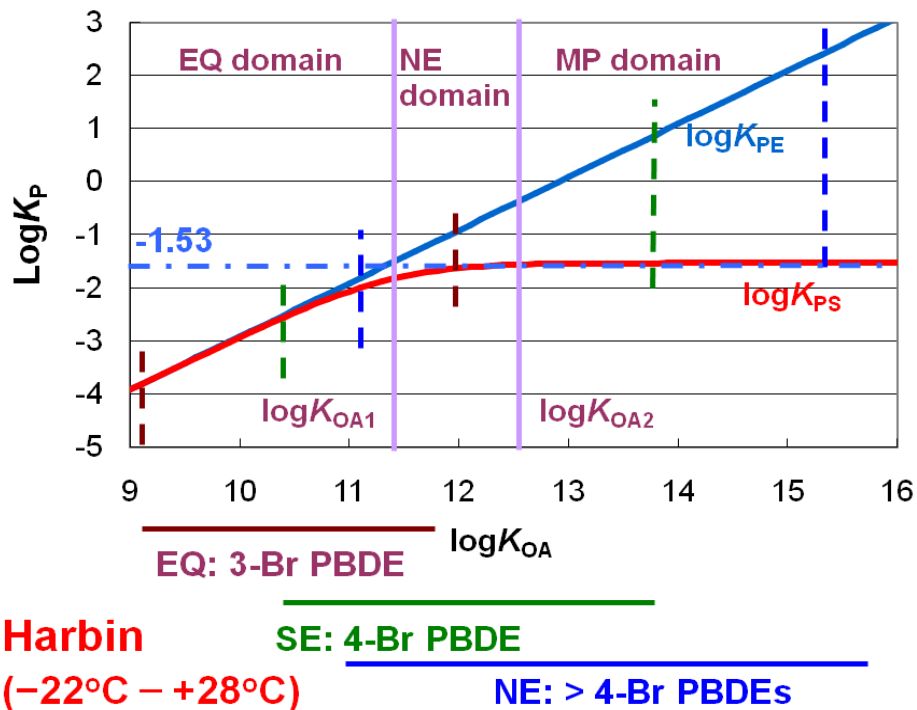
860

861 **Figure 3.** The range of $\log K_{OA}$ (the left axis) and the threshold temperatures (the right axis)
862 for 10 PBDE congeners in Harbin air at a temperature range of -22 $^{\circ}\text{C}$ to +28 $^{\circ}\text{C}$. The ranges
863 of $\log K_{OA}$ for the 10 PBDE congeners are given by the vertical bars. The 2 horizontal light
864 blue dashed lines give the 2 threshold values of $\log K_{OA1}$ and $\log K_{OA2}$, and the red diamonds
865 and red squares present respectively the two corresponding threshold temperatures, t_{TH1} and
866 t_{TH2} . The former divides the space of $\log K_{OA}$ (the left axis) and the later divides the
867 temperature space (the right axis) into three domains: the EQ domain, the NE domain, and
868 the MP domain. Thus the PBDE congeners (homologues) in Harbin air can be segregated
869 into 3 groups; BDE-17 and 28 (3-Br homologue) as equilibrium EQ-group, BDE-47 and 66
870 (4-Br homologue) as semiequilibrium SE-group, and others (>4-Br homologues) as
871 nonequilibrium NE-group.

872

873

874



875

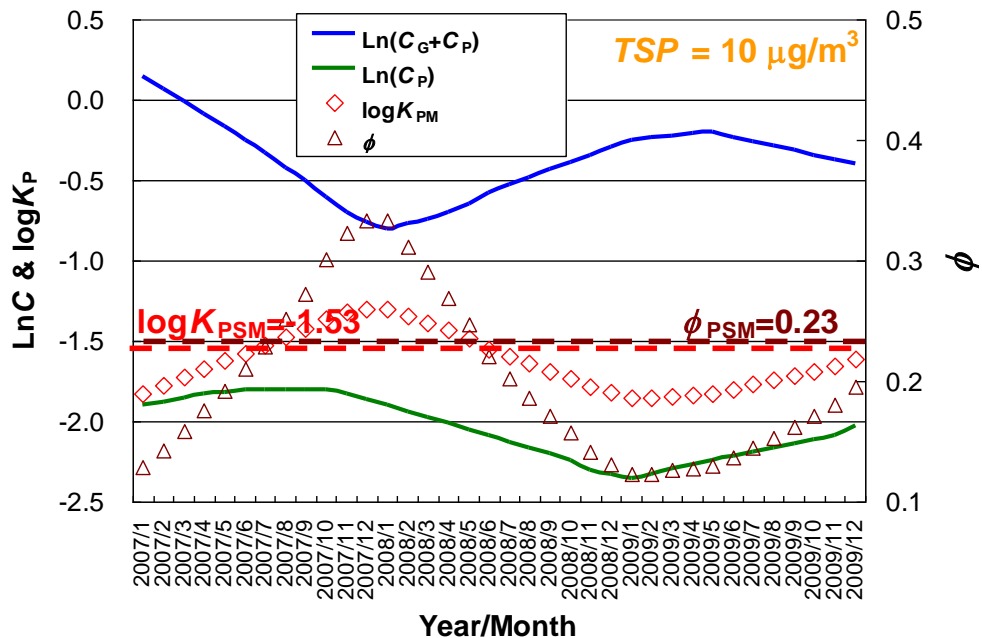
876

877 **Figure 4.** The $\log K_p$ - $\log K_{OA}$ diagram for the 10 PBDE congeners in Harbin air at a
 878 temperature range of -22 to +28 $^{\circ}\text{C}$. The EQ Group includes BDE-17 and -28, the SE Group
 879 contains BDE-47 and -66, and the rests belong to NE Group. The range of $\log K_{OA}$ for each
 880 group and their corresponding $\log K_p$ - $\log K_{OA}$ diagram are also shown. The $\log K_p$ - $\log K_{OA}$
 881 diagram for the EQ Group, boned by 2 purple dashed lines, is mainly in the EQ domain, with
 882 a small portion in NE domain; the $\log K_p$ - $\log K_{OA}$ diagram for the SE Group, contained by 2
 883 green dashed lines, is mainly in the NE domain, with a small portion in MP domain; and the
 884 $\log K_p$ - $\log K_{OA}$ diagram for the NE Group, formed by the 2 blue dashed lines, is mainly in the
 885 NE and MP domains.

886

887

888



889

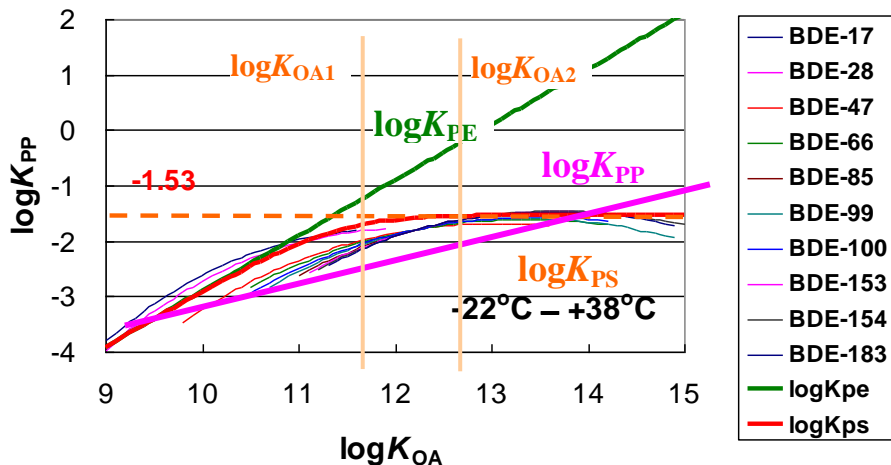
890 **Figure 5.** The temporal trends of concentrations of BDE-209 in the Arctic air in gas + particle
 891 phase (blue line) and in particle phase (green line) at Alert, Canada from 2007 to 2009 (NCP
 892 2013). The purple triangles and red diamonds are the values of ϕ and $\log K_p$ of BDE-209,
 893 respectively, calculated using the concentration data, and match well the values of ϕ_{PSM}
 894 ($=0.23$) and $\log K_{PSM}$ (-1.53), respectively ($TSP = 10 \mu\text{g m}^{-3}$ was assumed).

895

896

897

898



901 **Figure 6.** Variation of $\log K_{PS}$ (the thick red line, given by Eq. (31)), $\log K_{PE}$ (the thick dark
 902 green line, given by Eq. (3)), and $\log K_{PP}$ (the thick pink line, given by Eq. (6)) as functions of
 903 $\log K_{OA}$. The functions of $\log K_{PP}(K_{OA})$ (the thin lines, given by Eq. (8)) versus $\log K_{OA}$ for 10
 904 PBDE congeners in Harbin air at a temperature range of -22 to +28 $^{\circ}\text{C}$ are also included.